

Enhancing Quantization-Aware Training on Edge Devices via Relative Entropy Coreset Selection and Cascaded Layer Correction

Yujia Tong, Jingling Yuan, *Senior Member, IEEE*, Chuang Hu, *Member, IEEE*

Abstract—With the development of mobile and edge computing, the demand for low-bit quantized models on edge devices is increasing to achieve efficient deployment. To enhance the performance, it is often necessary to retrain the quantized models using edge data. However, due to privacy concerns, certain sensitive data can only be processed on edge devices. Therefore, employing Quantization-Aware Training (QAT) on edge devices has become an effective solution. Nevertheless, traditional QAT relies on the complete dataset for training, which incurs a huge computational cost. Coreset selection techniques can mitigate this issue by training on the most representative subsets. However, existing methods struggle to eliminate quantization errors in the model when using small-scale datasets (e.g., only 10% of the data), leading to significant performance degradation. To address these issues, we propose QuaRC, a QAT framework with coresets on edge devices, which consists of two main phases: In the coreset selection phase, QuaRC introduces the “Relative Entropy Score” to identify the subsets that most effectively capture the model’s quantization errors. During the training phase, QuaRC employs the Cascaded Layer Correction strategy to align the intermediate layer outputs of the quantized model with those of the full-precision model, thereby effectively reducing the quantization errors in the intermediate layers. Experimental results demonstrate the effectiveness of our approach. For instance, when quantizing ResNet-18 to 2-bit using a 1% data subset, QuaRC achieves a 5.72% improvement in Top-1 accuracy on the ImageNet-1K dataset compared to state-of-the-art techniques.

Index Terms—Quantization-Aware Training, edge computing, coreset selection, efficient training.

I. INTRODUCTION

WITH the rapid growth of mobile devices and edge computing, real-time computer vision tasks—such as scene classification [1] and crack detection [2]—are increasingly executed on smartphones, laptops, and Unmanned Aerial Vehicles (UAVs). These applications must run under stringent compute and battery limits [3], [4]. Although lightweight architectures like MobileNetV2 [5] reduce overhead, they still struggle to meet real-time latency targets on image data.

Model quantization [6], [7] addresses this gap by lowering the bitwidth of weights and activations, cutting both storage and arithmetic cost. Quantization splits into Post-Training Quantization (PTQ) [8], [9] and Quantization-Aware Training (QAT) [10], [11]. PTQ applies quantization to a trained

model without retraining, but accuracy degrades sharply at low bitwidths (≤ 4 bits). QAT, by simulating quantization effects during training, adapts the model to quantization noise and retains higher accuracy. As a result, QAT is the preferred route for aggressive bitwidth reduction on edge devices.

Conventional QAT pipelines, however, face many limitations in practical applications. To obtain a quantized model, traditional QAT usually involves transmitting data generated on the edge devices to the cloud, where the model is trained with quantization using this data. The quantized model is then transmitted back to the edge devices. However, due to data privacy and communication latency issues, data generated on edge devices often needs to be processed locally. Therefore, QAT needs to be performed directly on the edge devices. Traditional QAT methods require training with the entire dataset, which incurs significant computational and time overheads. This is unacceptable for edge devices. As a result, improving the efficiency of QAT on edge devices has become a critical research direction.

A promising strategy to mitigate the computational overhead of QAT is the utilization of *coreset* techniques [12]–[15]. These methods identify a representative subset of the dataset, creating a smaller yet statistically and structurally representative training set that closely approximates the original data. By applying coreset selection, the training process can be substantially accelerated, reducing computational costs while preserving the model’s performance and robustness.

Applying coresets to QAT poses two main challenges. First, *how to select samples that accurately capture quantization errors?* Quantization errors—introduced by reduced precision—directly drive accuracy loss. Existing coreset metrics (e.g., error vector score, disagreement score [16]) do not explicitly measure a sample’s contribution to quantization errors. Precise selection criteria are therefore needed to ensure the coreset highlights the most error-sensitive inputs.

Second, *how to retrain on a small coreset so as to minimize quantization error propagation?* Standard QAT losses, possibly augmented with knowledge distillation, work well on full datasets but falter on small subsets. Limited samples fail to correct accumulated errors in intermediate layers, leading to degraded performance. A tailored training strategy is required to suppress layer-wise quantization errors when data are scarce.

In this paper, we address two key challenges in coreset selection for QAT, aiming to mitigate the performance degradation of quantized models when using a small-scale coreset.

Yujia Tong, Jingling Yuan are with Hubei Key Laboratory of Transportation Internet of Things, School of Computer Science and Artificial Intelligence, Wuhan University of Technology, Hubei 430072, China. (E-mail: {tyjjij, yjl}@whut.edu.cn.)

Chuang Hu is with the School of Computer Science, Wuhan University, Hubei 430072, China. (E-mail: handc@whu.edu.cn.)

We propose QuaRC, a **Quantization-aware** training framework on edge devices via **Relative entropy** coreset selection and **Cascaded layer correction**. Specifically, during the coreset selection phase, we first input the same samples into both the full-precision model and the quantized model, and calculate the difference in their outputs using relative entropy. We find that samples with higher relative entropy are more capable of capturing quantization errors, and training with such samples can improve model accuracy. To verify this phenomenon, we test the impact of samples with different relative entropies on the accuracy of quantized models and calculate the Spearman correlation coefficient between relative entropy and model performance. The results show a strong correlation between the two. Based on this observation, we propose the **Relative Entropy Score (RES)** as a criterion for coreset selection. In the quantized model training phase, to address the accumulation of quantization errors across layers, we introduce a **Cascaded Layer Correction (CLC)** strategy. This approach aligns the intermediate layer outputs of the quantized model with those of the full-precision model, thereby reducing errors at intermediate layers. We conduct extensive experiments to validate our method. Compared to previous methods, our approach can significantly enhance the performance of the quantized model when selecting a small-scale coreset (10% or less) for QAT.

In summary, our contributions are:

- We propose a new metric for coreset selection—Relative Entropy Score (RES). This metric can be used to select the samples that accurately capture quantization errors.
- We propose the Cascaded Layer Correction (CLC) training strategy that can effectively eliminate the quantization errors in the intermediate layers of the model.
- We conduct extensive experiments to validate our method. Compared to previous methods, our approach can significantly enhance the performance of the quantized model when training with a small-scale coreset (10% or less).
- To further demonstrate the effectiveness of QuaRC in the practical scenario, we conduct a case study on an unmanned aerial vehicle (UAV) for concrete crack detection.

II. BACKGROUND AND MOTIVATION

In this section, we first introduce the background of QAT. Subsequently, we discuss the challenges of existing coreset selection methods when applied to QAT, which motivates our proposed method.

A. Quantization-Aware Training

To simulate the rounding and clamping errors of the quantized model during the inference process, QAT [17], [18] introduces fake quantization nodes that perform quantization and dequantization operations on floating-point numbers. For n -bit signed quantization, given a scaling factor s , the full-precision number x^r is converted to x^q at the fake quantization node through quantization and dequantization operations:

$$x^q = q(x^r) = s \times \left\lfloor \text{clamp} \left(\frac{x^r}{s}, -Q_N, Q_P \right) \right\rfloor \quad (1)$$

where $\lfloor \cdot \rfloor$ is an operation used to round its input to the nearest integer. The function $\text{clamp}(x, r_{\text{low}}, r_{\text{high}})$ returns x while ensuring that values below r_{low} are set to r_{low} , and values above r_{high} are set to r_{high} .

Typically, in a neural network where both activations and weights are quantized, the forward and backward propagation processes can be simply represented as:

$$\begin{aligned} \text{Forward: } \text{Output}(x) &= x^q \cdot w^q = q(x^r) \cdot q(w^r) \\ \text{Backward: } \frac{\partial \mathcal{J}}{\partial x^r} &= \begin{cases} \frac{\partial \mathcal{J}}{\partial x^q} & \text{if } x \in [-Q_N^x, Q_P^x] \\ 0 & \text{otherwise} \end{cases} \\ \frac{\partial \mathcal{J}}{\partial \mathbf{w}^r} &= \begin{cases} \frac{\partial \mathcal{J}}{\partial \mathbf{w}^q} & \text{if } \mathbf{w} \in [-Q_N^w, Q_P^w] \\ 0 & \text{otherwise} \end{cases} \end{aligned} \quad (2)$$

where \mathcal{J} is the loss function, $q(\cdot)$ is employed during forward propagation, and the straight-through estimator (STE) [19] is utilized to maintain the derivation of the gradient during backward propagation.

In image classification tasks [20], neural networks primarily extract features and enable effective classification. We can regard this process as a transformation from input data to output results. Specifically, the workflow entails mapping the input image x to the predicted probability distribution $p(w, x)$ via the forward propagation function $f(w, x)$ of the neural network, where w denotes the network's weight parameters. For any sample (x, y) in the coreset, we input it into both the full-precision and quantized models. The resulting output probability distributions (logits) are represented by:

$$p_F(w^r, x^r) = f(w^r, x^r), p_Q(w^q, x^q) = f(w^q, x^q) \quad (3)$$

In QAT, a significant challenge is reducing quantization errors, which propagate and accumulate in the deeper layers of the model. Knowledge distillation (KD), when applied to QAT, can reduce quantization errors of quantized models [21]–[24]. Typically, the full-precision model acts as the teacher, and the quantized model acts as the student. The objective of the KD loss function is to minimize the disparity between the output distributions of the final layer of the full-precision model and the quantized model. This is achieved through the following formulation:

$$\mathcal{L}_{KD} = - \sum_m p_{\mathbf{T}}^{(m)}(w^r, x_i) \log(p_{\mathbf{Q}}^{(m)}(w^q, x_i)) \quad (4)$$

where \mathcal{L}_{KD} is the KD loss function, defined as the cross-entropy between the output distributions $p_{\mathbf{T}}$ and $p_{\mathbf{Q}}$ of the full-precision teacher model and the quantized student model, and m denotes the classes. The teacher model can be a full-precision model corresponding to the quantized model, or it can be a full-precision model of the same type with a deeper number of layers.

However, traditional QAT requires retraining the quantized model using the entire dataset, which leads to substantial computational resources and time overhead. For example, even with a small dataset like CIFAR-100, the QAT of MobileNetV2 takes 75.22 minutes, which is unacceptable for edge devices. Therefore, enhancing the efficiency of QAT is critical.

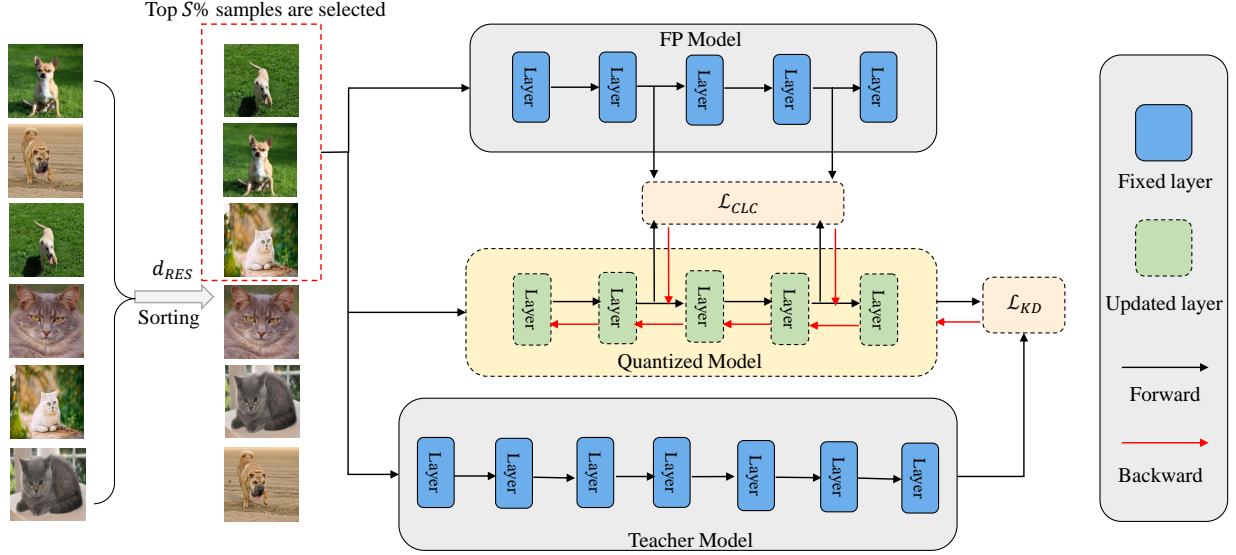


Fig. 1: The overview of QuaRC.

B. Coreset Selection for QAT

Coreset selection techniques can enhance the efficiency of QAT by identifying the most representative subsets for training. However, most existing coreset selection methods are designed for full-precision models and do not account for the unique characteristics of quantized models. For instance, classical methods such as Moderate [25], Contextual Diversity (CD) [26], and Forgetting [27] rely on various criteria to select samples. Moderate and CD use geometry-based criteria to select samples that can approximate the distribution of the full dataset, while Forgetting focuses on the frequency of forgetting events to identify samples that are more difficult to learn and potentially more informative for training. While these methods perform well for full-precision models, their performance in QAT is even worse than that of random sampling.

Recent work like ACS [16] attempts to bridge this gap by introducing metrics such as the error vector score and disagreement score. These metrics aim to identify the samples that contribute the most to the parameter updates of the quantized model. However, they fail to consider the correlation between samples and quantization errors, which can be explicitly manifested as the differences between the output logits of full-precision and quantized models.

C. Challenge and Motivation

Quantization errors primarily originates from two sources: 1) the rounding and clamping operations during fake quantization, which distort the forward propagation of activations and weights, as reflected in Eq.(1), and 2) the use of STE during backpropagation, which introduce approximation errors in gradient updates, as reflected in Eq.(2). Existing coreset selection criteria fail to prioritize samples that expose these errors during QAT, thereby limiting the model's ability to adapt to quantization noise.

Moreover, quantization errors accumulate and propagate through the intermediate layers of the model. To mitigate these

errors, existing QAT methods employ KD strategies during training. However, traditional KD methods focus solely on optimizing the final output. When training with the full dataset, the large volume of data can effectively eliminate the errors in the intermediate layers of the quantized model. But when the coreset size is small (e.g., 10% of the dataset), even using KD strategies fails to eliminate the errors in the intermediate layers of the quantized model.

The above challenges motivate us to design: 1) a coreset selection method that can **reflect the quantization errors** of the model, and 2) a training strategy that can **eliminate the quantization errors** of the model.

III. DESIGN OF QUARC

In this section, we first introduce the overview of our method—QuaRC. Subsequently, we describe two key phases of QuaRC: the coreset selection phase and the quantized model training phase.

A. Overview of QuaRC

As shown in Fig. 1, QuaRC is a framework that utilizes coresets for QAT, which mainly consists of two phases:

① *Coreset Selection Phase*: In this phase, we aim to select a small yet representative subset of the dataset that can effectively capture the quantization errors of the model. We propose the **Relative Entropy Score (RES)** as the criterion for selecting the coreset. Specifically, we input each sample into both the full-precision model and the quantized model, and calculate the relative entropy between their output distributions. Samples with higher relative entropy are considered more capable of capturing the quantization errors. Therefore, we sort all samples based on their relative entropy scores and select the top $S\%$ samples to form the coreset. This coreset will be used for training the quantized model in the next phase.

② *Quantized Model Training Phase*: In this phase, we train the quantized model using the selected coreset. To address

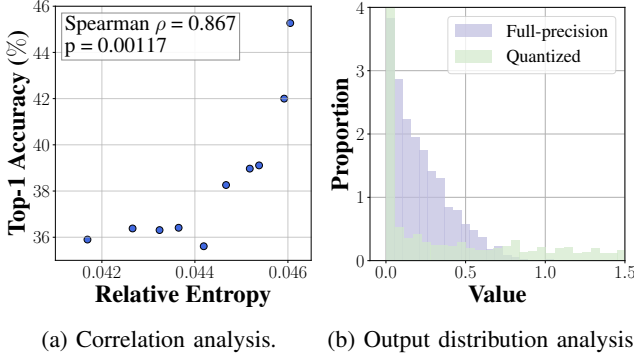


Fig. 2: (a) We select coresets with different mean values of relative entropy for training. (b) We compare the differences in intermediate layer outputs between the quantized model and the full-precision model. These observations are from training quantized MobileNetV2 on 1% of CIFAR-100 dataset.

the accumulation of quantization errors in the intermediate layers of the quantized model, we introduce a **Cascaded Layer Correction (CLC)** strategy. This strategy aligns the output distributions of the intermediate layers of the quantized model with those of the full-precision model by minimizing the Kullback-Leibler (KL) divergence between them. Specifically, we add an additional loss term to the training objective, which encourages the quantized model to learn representations that are closer to those of the full-precision model at each intermediate layer. This helps to reduce the quantization errors and improve the overall accuracy of the quantized model.

We will describe these two phases in detail in Section III-B and Section III-C.

B. Relative Entropy Coreset Selection Phase

Quantization Errors Analysis. Although existing coreset selection methods have improved the efficiency of QAT, selecting a small-scale coreset for training often leads to a significant drop in the performance of the quantized model. This is because these methods do not directly select the coreset from the perspective of reducing model quantization errors, making it difficult to eliminate such errors in subsequent training. To reduce the model’s quantization errors, it is essential to ensure that the selected coreset can reflect those errors.

Quantization errors manifest as the discrepancy between the outputs of the full-precision model $p_F(w^r, x^r)$ and its quantized counterpart $p_Q(w^q, x^q)$ for the same input sample (x, y) . Minimizing this discrepancy is the core objective of QAT (Eq.(4)). We can use relative entropy to measure the difference between these two outputs. When the relative entropy is small, it indicates that the output of the quantized model $p_Q(w^q, x^q)$ is very similar to the output of the full-precision model $p_F(w^r, x^r)$. This means that the sample hardly captures the errors in the quantized model. In this case, training with such samples results in a small loss value that is close to convergence, leading to very limited updates to the model parameters. Consequently, it is difficult to effectively reduce the quantization errors. Conversely, when the relative entropy is large, it indicates a significant difference between

$p_Q(w^q, x^q)$ and $p_F(w^r, x^r)$. Training with such samples results in a larger loss value, allowing for substantial updates to the model parameters, thereby effectively reducing the quantization errors.

Furthermore, we select 10 coresets with different relative entropies from the full dataset (the relative entropy of a coreset is defined as the average relative entropy of the samples it contains), with each coreset containing 1% of the samples from the full dataset. We then train 2-bit quantized MobileNetV2 models using these coresets and obtain the Top-1 accuracy of the models, as shown in Fig. 2(a). The Spearman correlation coefficient between relative entropy and Top-1 accuracy is 0.867, with $p = 0.00117 < 0.05$, indicating a significant and strong positive correlation between these two variables. This experiment further demonstrates that using relative entropy as a metric for coreset selection can effectively reflect the model’s quantization errors, helping to reduce these errors during training and thereby improving the model’s performance.

Relative Entropy Score. Based on the above insights, we propose the Relative Entropy as the metric for coreset selection. Before training the quantized model, we first traverse every sample in the dataset, and input each sample into both the quantized model and the full-precision model to obtain two outputs $p_Q^{(m)}(w^q, x^q)$ and $p_F^{(m)}(w^r, x^r)$. Then, calculate the Relative Entropy Score (RES) according to the following formula:

$$d_{\text{RES}} = \sum_m p_Q^{(m)}(w^q, x^q) \log \left(\frac{p_Q^{(m)}(w^q, x^q)}{p_F^{(m)}(w^r, x^r)} \right) \quad (5)$$

where m denotes the classes.

Final Selection Metric. The metrics $d_{\text{EVS}} = \|p(w_t^q, x) - y\|_2$ and $d_{\text{DS}} = \|p(w_t^q, x) - p_T(w_t^r, x)\|_2$ select the coreset from the perspective of gradients. Using the cosine annealing weight coefficient $\alpha(t) = \cos(\frac{t}{2T}\pi)$, based on the current training epoch t and the total number of training epochs T , to balance them can select the coreset that contributes the most to model training, thereby maximizing model performance [16]. Unlike these two metrics, d_{RES} selects the samples that best reflect the model’s quantization errors as the coreset for training, maximizing model performance from the perspective of reducing quantization errors. We select the coreset from both the gradient and quantization error perspectives, combining the above three metrics as the final coreset selection metric:

$$d_S(t) = \alpha(t)d_{\text{EVS}}(t) + (1 - \alpha(t))d_{\text{DS}}(t) + d_{\text{RES}}(t) \quad (6)$$

We sort the samples in the entire dataset based on $d_S(t)$ and select the top $S\%$ of samples for subsequent training.

C. Cascaded Layer Correction Training Phase

Intermediate Layer Errors Analysis. Training with KD on the full dataset can alleviate the accuracy drop of the quantized model. However, when training with a small coreset, it can lead to a significant decrease in the accuracy of the quantized model. To explore the reasons, we evaluate whether the model’s learning and representation abilities for samples changed during the quantization process. Specifically, we input the same samples into the full-precision model and the 3-bit

Algorithm 1 The overall pipeline of QuaRC

Input: Training dataset $D = \{(x_i, y_i)\}_{i=1}^n$, Initial coreset $D_S(t)$, Coreset data fraction S , Total training epochs T , Selection interval R , FP model's weights \mathbf{W}^r
Output: Quantized model's weights \mathbf{W}^q
 Initialize quantized weights \mathbf{W}^q following Eq.(1)
for $t \in [0, \dots, T - 1]$ **do**
 # Stage 1: Coreset selection
 if $t \% R == 0$ **then**
 for $(x_i, y_i) \in D$ **do**
 Calculate $d_{\text{EVS}}(x_i, t)$ and $d_{\text{DS}}(x_i, t)$
 Calculate $d_{\text{RES}}(x_i, t)$ by Eq.(5)
 Combine the scores to obtain $d_S(x_i, t)$ by Eq.(6)
 end for
 Sort $d_S(x_i, t)$, choose top $S\%$ samples as $D_S(t)$
 else
 $D_S(t) \leftarrow D_S(t - 1)$
 end if
 # Stage 2: Model training
 Calculate \mathcal{L}_{KD} by Eq.(4) and \mathcal{L}_{CLC} by Eq.(8)
 Combine the losses by Eq.(9) and train \mathbf{W}^q on $D_S(t)$ following Eq.(9)
end for

quantized model trained using the KD strategy. Throughout the forward propagation, we capture and record outputs from the intermediate layers, with the output distributions depicted in Fig. 2(b). We find that the inter-layer output distributions of the quantized model and the full-precision model differ significantly. Specifically, the KL divergence between the inter-layer outputs of the 3-bit quantized model and the full-precision model is $9.0\text{e-}4$, which indicates that the errors in the intermediate layers of the quantized model are difficult to eliminate.

Cascaded Layer Correction. In common KD training strategies (i.e., optimizing only the output distribution of the last layer), the entire dataset is used for training. Extensive data training can reduce the quantization errors in the model's intermediate layers. However, training with a small-scale coreset is not sufficient to eliminate errors in the intermediate layers. Therefore, it is necessary to design strategies to optimize the output distribution of the intermediate layers, ensuring that the quantized model maintains a representation ability close to that of the full-precision model at intermediate layers [28].

To minimize the difference between the intermediate layer outputs of the full-precision and quantized models, we propose a Cascaded Layer Correction (CLC) training strategy. Specifically, we use a full-precision correction model to adjust the output distribution of selected intermediate layers of the quantized model. This adjustment is guided by the following formula:

$$\min \sum \text{distance}(O, \hat{O}) \quad (7)$$

where O represents the output distribution of selected intermediate layers from the full-precision model, and \hat{O} denotes the output distribution of the corresponding selected intermediate layers from the quantized model. We utilize information dis-

tance to measure the distance between output distributions, and reducing the difference in the output of the intermediate layer between the full-precision model and the quantized model is equivalent to optimizing the following loss function in training:

$$\mathcal{L}_{\text{CLC}} = \sum_c p_{\mathbf{Q}}^i(w^q, x^q) \log \left(\frac{p_{\mathbf{Q}}^i(w^q, x^q)}{p_{\mathbf{F}}^i(w^r, x^r)} \right) \quad (8)$$

where c represents the intermediate layer to be optimized, $p_{\mathbf{Q}}^i(w^q, x^q)$ and $p_{\mathbf{F}}^i(w^r, x^r)$ denote outputs of the intermediate layer.

Total Training Loss. We use both KD and CLC for QAT, and the final loss function is as follows:

$$\mathcal{L}_{\text{TOTAL}} = \mathcal{L}_{\text{KD}} + \beta \mathcal{L}_{\text{CLC}} \quad (9)$$

To help better understand the training process, we provide the brief pseudo-code of it in Algorithm 1. Following ACS [16], we perform coreset selection every R epoch, where R is predetermined prior to the training.

IV. THEORETICAL ANALYSIS

In this section, we first conduct a theoretical analysis of the computational complexity of QuaRC and demonstrate that it can improve the training efficiency of QAT. Subsequently, we provide a convergence analysis for QAT using coresets.

A. Complexity Analysis

We theoretically prove that QuaRC can improve the efficiency of QAT. In traditional QAT, the model performs one forward pass and one backward pass on the entire dataset in each training epoch. Assuming the dataset contains N samples, the number of training epochs is T , the complexity of the forward pass is $O(F)$, and the complexity of the backward pass is $O(B)$, the total time complexity of traditional QAT is $O(T \cdot N \cdot (F + B))$.

QuaRC selects a small subset of samples for training using a coreset. Assuming the selected sample ratio is S (e.g., $S = 0.01$ represents selecting 1% of the samples), the complexity of the forward and backward passes per epoch is reduced to $O(S \cdot N \cdot (F + B))$. Therefore, the complexity of the coreset-based training is $O(T \cdot S \cdot N \cdot (F + B))$. RES requires two additional forward passes to compute the relative entropy. For each sample in the dataset, these two forward passes are performed. The computational complexity of calculating the relative entropy is negligible compared to forward propagation. Assume that coreset selection is performed every R rounds. Thus, the computational complexity of RES is $O(2 \cdot F \cdot N \cdot T/R)$. The introduction of CLC mainly involves adding an additional loss term to optimize the output distribution of intermediate layers. The computational complexity of CLC is negligible and already included in the complexity of the forward pass. By summing up the above complexities, the total time complexity of QuaRC is $O(T \cdot S \cdot N \cdot (F + B)) + O(2 \cdot F \cdot N \cdot T/R)$. Since $O(B) > O(F)$ [29], when S is sufficiently small (e.g., $S < 0.1$), the following equation holds:

$$O(T \cdot N \cdot (F+B)) \gg O(T \cdot S \cdot N \cdot (F+B)) + O(2 \cdot F \cdot N \cdot T/R) \quad (10)$$

Through the above theoretical analysis, it can be proven that using our method can improve the efficiency of QAT.

B. Convergence Analysis

We analyze the convergence of QAT with coresets. For the coreset D_S and the loss function $\mathcal{L}(w^q; D_S)$, we assume that:

- 1) *Assumption 1:* The loss function $\mathcal{L}(w^q; D_S)$ is Lipschitz-smooth which implies that there exists a constant $L > 0$ such that for all $w^q, w^{q'} \in \mathbb{R}^d$ and any sample $d \in D_S$,

$$\|\nabla \mathcal{L}(w^q; d) - \nabla \mathcal{L}(w^{q'}; d)\| \leq L \|w^q - w^{q'}\| \quad (11)$$

- 2) *Assumption 2:* The gradient $\nabla \mathcal{L}(w^q; d)$ is bounded, i.e., there exists a constant G such that for all $w^q \in \mathbb{R}^d$ and $d \in D_S$ we have

$$\|\nabla \mathcal{L}(w^q; d)\| \leq G \quad (12)$$

- 3) *Assumption 3:* The learning rate η_t satisfies

$$\sum_{t=1}^{\infty} \eta_t = \infty \quad \text{and} \quad \sum_{t=1}^{\infty} \eta_t^2 < \infty \quad (13)$$

Stochastic gradient descent (SGD) is employed for optimization. To simplify the proof, the weights can be updated according to the following equation:

$$w_{t+1}^q = w_t^q - \eta_t g_t \quad (14)$$

where $g_t = \nabla \mathcal{L}(w_t^q; d)$ and $d \in D_S$.

Lemma 1. For any iteration t and $d \in D_S$, the loss difference satisfies:

$$\mathcal{L}(w_{t+1}^q; d) - \mathcal{L}(w_t^q; d) \leq -\eta_t \left(1 - \frac{L\eta_t}{2}\right) \|g_t\|^2 \quad (15)$$

Proof. Expand $\mathcal{L}(w_{t+1}^q; d)$ using Taylor series around w_t^q :

$$\begin{aligned} \mathcal{L}(w_{t+1}^q; d) &= \mathcal{L}(w_t^q; d) + \nabla \mathcal{L}(w_t^q; d)^T (w_{t+1}^q - w_t^q) \\ &\quad + \frac{1}{2} (w_{t+1}^q - w_t^q)^T \nabla^2 \mathcal{L}(c) (w_{t+1}^q - w_t^q) \end{aligned} \quad (16)$$

where c lies between w_t^q and w_{t+1}^q . Substitute $w_{t+1}^q - w_t^q = -\eta_t g_t$ and use *Assumption 1*:

$$\begin{aligned} \mathcal{L}(w_{t+1}^q; d) &\leq \mathcal{L}(w_t^q; d) - \eta_t \|g_t\|^2 + \frac{1}{2} \eta_t^2 L \|g_t\|^2 \\ &= \mathcal{L}(w_t^q; d) - \eta_t \left(1 - \frac{L\eta_t}{2}\right) \|g_t\|^2 \end{aligned} \quad (17)$$

□

Lemma 2. The sequence $\{\mathbb{E}[\mathcal{L}(w_t^q; d)]\}$ is non-increasing:

$$\mathbb{E}[\mathcal{L}(w_{t+1}^q; d)] \leq \mathbb{E}[\mathcal{L}(w_t^q; d)] \quad (18)$$

Proof. Take expectations in Lemma 1 and use *Assumption 2*:

$$\mathbb{E}[\mathcal{L}(w_{t+1}^q; d) - \mathcal{L}(w_t^q; d)] \leq -\eta_t \left(1 - \frac{L\eta_t}{2}\right) \mathbb{E}[\|g_t\|^2] \quad (19)$$

From *Assumption 3*, $\eta_t \in [0, 2/L]$ for large t , thus:

$$\mathbb{E}[\mathcal{L}(w_{t+1}^q; d)] \leq \mathbb{E}[\mathcal{L}(w_t^q; d)] \quad (20)$$

□

Theorem 1. Under *Assumptions 1-3*, the sequence $\{\mathbb{E}[\mathcal{L}(w_t^q; d)]\}$ converges to a limit $L^* \geq 0$.

Proof. From Lemma 2, the sequence $\{\mathbb{E}[\mathcal{L}(w_t^q; d)]\}$ is:

- Non-increasing: $\mathbb{E}[\mathcal{L}(w_{t+1}^q; d)] \leq \mathbb{E}[\mathcal{L}(w_t^q; d)]$
- Lower bounded by 0: $\mathcal{L}(w_t^q; d) \geq 0$ (by definition of loss functions)

By the Monotone Convergence Theorem, there exists $L^* \geq 0$ such that:

$$\lim_{t \rightarrow \infty} \mathbb{E}[\mathcal{L}(w_t^q; d)] = L^* \quad (21)$$

□

Therefore, the sequence $\{\mathbb{E}[\mathcal{L}(w_t^q; d)]\}_{t=1}^{\infty}$ is non-increasing and lower-bounded, so it must converge to some limit L^* , signifying the convergence of QAT with coresets.

V. EXPERIMENTS

A. Experimental Setup

Datasets and Networks. The datasets used in our experiments are CIFAR-100 [30] and ImageNet-1K [31]. We apply data augmentation techniques, *RandomResizedCrop* and *RandomHorizontalFlip*, provided by PyTorch [32]. Consistent with ACS [16], we evaluate our method on two widely-used neural networks: MobileNetV2 [5] and ResNet-18 [33].

Baselines. Our work focuses on addressing performance degradation in quantized models using small-scale coresets for QAT. Therefore, we selected baselines related to coreset selection, rather than QAT methods that modify the training strategy without addressing coreset selection. To ensure a fair comparison, we have selected multiple baselines for comparison, which can be categorized as follows:

- Random Sampling: Randomly select a coreset of specified size from each class for QAT.
- Forgetting [27]: Select samples based on early training forgetting statistics, focusing on those triggering more forgetting events and being more challenging to learn, as the coreset for QAT.
- ContextualDiversity(CD) [26]: Choose the centroids of sample clusters as the coreset for QAT.
- Moderate [25]: Select samples with scores close to the median score as the coreset for QAT.
- ACS [16]: Adaptively select samples with the greatest impact on gradients as the coreset for QAT at different intervals.

Metrics. We use Top-1 and Top-5 accuracy as evaluation metrics. For inference, we report the Top-1 and Top-5 accuracy of the full-precision models. Specifically, the full-precision MobileNetV2 achieves 72.56% Top-1 and 91.93% Top-5 accuracy on CIFAR-100, while the full-precision ResNet-18 achieves 69.76% Top-1 and 89.07% Top-5 accuracy on ImageNet-1K.

TABLE I: Comparison of Top-1 and Top-5 accuracy of different methods on QAT of quantized MobileNetV2 on CIFAR-100 with different subset fractions. The bitwidth for quantized MobileNetV2 is 2/32, 3/32, and 4/32 for weights/activations.

Method	Bit Width	1%		3%		5%		7%		10%	
		Top-1	Top-5	Top-1	Top-5	Top-1	Top-5	Top-1	Top-5	Top-1	Top-5
Random	2w32a	40.57	71.74	53.22	80.43	56.21	83.45	59.52	85.73	60.81	86.42
Forgetting [27]		40.73	70.69	51.90	80.04	55.78	83.27	58.26	84.36	60.39	86.01
CD [26]		38.61	68.30	51.53	79.36	55.13	82.55	57.86	83.63	58.53	85.05
Moderate [25]		35.14	65.47	48.99	77.86	51.99	80.91	55.17	83.31	57.51	84.02
ACS [16]		46.84	78.09	57.07	84.64	59.59	85.95	61.59	87.54	63.32	87.71
QuaRC (Ours)		56.36	85.08	61.97	87.66	63.30	88.01	64.19	88.62	65.64	88.98
Random	3w32a	62.93	86.89	65.59	88.86	67.58	89.72	68.15	90.34	69.08	90.34
Forgetting [27]		63.01	86.45	65.43	89.44	67.58	89.41	68.18	89.85	68.77	90.86
CD [26]		62.10	86.31	66.16	88.50	67.24	89.24	68.52	89.81	68.77	90.41
Moderate [25]		61.71	86.19	65.29	88.26	67.00	89.41	67.57	89.97	67.88	90.07
ACS [16]		64.98	88.64	67.83	90.11	68.48	90.58	68.94	91.22	69.13	90.59
QuaRC (Ours)		68.69	90.89	69.41	91.27	70.11	91.77	70.23	91.35	70.99	91.60
Random	4w32a	69.21	90.55	70.17	91.28	70.68	91.10	70.94	91.31	71.28	91.80
Forgetting [27]		69.35	90.38	70.19	91.12	70.47	91.35	71.12	91.51	71.18	91.84
CD [26]		69.03	90.41	70.35	91.04	70.53	91.16	71.05	91.58	71.30	91.29
Moderate [25]		68.69	90.11	70.30	90.74	70.40	91.15	70.86	91.06	71.02	91.34
ACS [16]		69.37	90.68	70.55	91.30	70.92	91.50	71.26	91.53	71.39	91.83
QuaRC (Ours)		71.25	91.39	71.53	91.64	71.86	91.73	71.98	91.72	72.03	91.94

Implementation Details. Following ACS [16], we use the quantization method from LSQ+ [34]. For MobileNetV2 on CIFAR-100, we train for 200 epochs with a learning rate of 0.01, weight decay of $5e-4$, batch size of 256, and the SGD optimizer, setting $R = 50$ and $\beta = 1e5$. The teacher model is MobileNetV2. For ResNet-18 on ImageNet-1K, we train for 120 epochs with a learning rate of $1.25e-3$, no weight decay, batch size of 128, and the Adam optimizer, setting $R = 10$ and $\beta = 3e3$. The teacher model is ResNet-101. All experiments are conducted on an NVIDIA RTX 4090 GPU.

B. Main Results

We present the Top-1 and Top-5 accuracy for MobileNetV2 on CIFAR-100 and ResNet-18 on ImageNet-1K in Table I and Table II. For MobileNetV2 on CIFAR-100, we quantize the weights to 2/3/4-bit, with activations remaining in full-precision. Specifically, when the weights are quantized to 2-bit, random sampling achieves a Top-1 accuracy of only 40.57% on a 1% subset. Other methods such as Forgetting, CD, and Moderate perform even worse, with accuracies of 40.73%, 38.61%, and 35.14%, respectively, all falling below the baseline level of random selection. This indicates that these methods fail to account for the characteristics of quantization and are not suitable for QAT. ACS, which employs a gradient-based dynamic balancing strategy, improves performance to 46.84%, but there is still a significant gap compared to the full-precision model’s accuracy of 72.56%. In contrast, our proposed QuaRC achieves a Top-1 accuracy of 56.36% on the 1% subset, representing an absolute improvement of 9.52% over ACS. This fully demonstrates its effectiveness in reducing quantization errors. As the quantization bitwidth increases to 3-bit and 4-bit, QuaRC continues to maintain a significant advantage. Specifically, on the 1% subset, QuaRC achieves Top-1 accuracies of 68.69% and 71.25%, respectively, which are significantly higher than ACS’s 64.98% and 69.37%. Moreover, QuaRC also shows excellent performance

on higher subset proportions (such as 5% and 10%), with Top-1 accuracies reaching 63.30% and 65.64% under 2-bit setting, respectively. This further proves the robustness and effectiveness of the QuaRC under different data scales.

For ResNet-18 on ImageNet-1K, we quantize both weights and activations to 2/3/4-bit. On large-scale datasets, QuaRC also demonstrates significant advantages. Specifically, under the setting of 2-bit weight and activation quantization, random sampling achieves a Top-1 accuracy of only 29.12% on a 1% subset. Other methods such as Forgetting and CD, due to their insufficient sample representativeness, further degrade performance, with the Moderate method’s accuracy dropping to 22.29%. The ACS method improves performance to 40.62%, but there is still a significant issue of error accumulation. QuaRC achieves a Top-1 accuracy of 46.34% on the 1% subset, representing an absolute improvement of 5.72% over ACS. This validates the synergistic effect of the quantization-aware coreset selection and cascaded layer correction strategies. As the subset proportion increases to 10%, the method maintains a stable performance of 62.32% under 2-bit quantization. Moreover, under quantization settings of 3-bit and 4-bit, QuaRC achieves absolute improvements of 2.82% and 1.47% over ACS on the 1% subset, respectively. These results comprehensively demonstrate the advantages of QuaRC.

As the bitwidth and subset fraction increase, the performance enhancement of the quantized model using our method diminishes. This occurs because larger bitwidth and subset fraction bring the performance of the quantized model closer to that of the full-precision model, making additional improvements more challenging. In general, our method can improve the performance of quantized models under various bitwidths and subset fractions, and the experiments have validated the superiority of our method.

TABLE II: Comparison of Top-1 and Top-5 accuracy of different methods on QAT of quantized ResNet-18 on ImageNet-1K with different subset fractions. The bitwidth for quantized ResNet-18 is 2/2, 3/3, and 4/4 for weights/activations.

Method	Bit Width	1%		3%		5%		7%		10%	
		Top-1	Top-5	Top-1	Top-5	Top-1	Top-5	Top-1	Top-5	Top-1	Top-5
Random	2w2a	29.12	53.95	45.60	71.09	51.28	75.89	54.59	78.58	57.44	80.76
Forgetting [27]		30.13	54.86	45.45	70.10	50.42	74.29	52.92	76.49	56.15	79.20
CD [26]		25.85	50.20	43.62	69.45	49.99	75.52	54.09	78.62	57.33	81.13
Moderate [25]		22.29	45.77	40.68	67.43	47.39	73.55	51.74	77.17	55.56	79.98
ACS [16]		40.62	65.60	53.68	77.22	57.39	80.51	59.76	82.41	61.55	83.44
QuaRC (Ours)		46.34	71.08	56.22	79.46	59.81	82.50	61.31	83.50	62.32	84.11
Random	3w3a	48.39	73.88	57.02	80.64	59.58	82.35	60.97	83.65	62.49	84.60
Forgetting [27]		48.13	73.09	55.77	79.26	58.60	81.14	60.16	82.41	61.42	83.23
CD [26]		46.78	72.75	56.20	80.43	59.09	82.68	60.74	83.76	62.39	84.72
Moderate [25]		45.10	72.02	54.68	79.57	57.77	81.72	59.46	82.86	61.05	84.02
ACS [16]		58.39	81.30	63.18	84.79	64.51	85.82	65.47	86.63	65.99	86.98
QuaRC (Ours)		61.21	83.21	64.49	85.59	65.40	86.22	65.67	86.66	66.19	86.81
Random	4w4a	56.59	80.45	60.89	83.53	62.80	84.73	63.78	85.38	64.47	86.03
Forgetting [27]		55.97	79.75	59.98	82.51	62.06	83.72	63.08	84.41	64.03	85.15
CD [26]		56.26	80.32	60.40	83.38	62.40	84.88	63.68	85.81	64.72	86.25
Moderate [25]		54.87	79.85	59.43	83.28	61.33	84.29	62.58	85.01	63.60	85.80
ACS [16]		63.83	85.19	66.41	87.04	67.29	87.74	67.76	87.92	68.23	88.34
QuaRC (Ours)		65.70	86.31	67.21	87.54	67.42	87.77	67.81	87.77	68.30	88.09

TABLE III: Evaluating RES and CLC of our method. We report the Top-1 and Top-5 accuracy of quantized MobileNetV2 on CIFAR-100. The baseline is ACS.

Method	Bit width	Fraction	Top-1	Top-5
Baseline	2w32a	1%	46.84	78.09
+RES	2w32a	1%	48.77	78.94
+CLC	2w32a	1%	55.25	84.03
+RES+CLC	2w32a	1%	56.36	85.08
Baseline	3w32a	1%	64.98	88.64
+RES	3w32a	1%	65.90	89.29
+CLC	3w32a	1%	68.32	90.53
+RES+CLC	3w32a	1%	68.69	90.89
Baseline	4w32a	1%	69.37	90.68
+RES	4w32a	1%	69.57	90.77
+CLC	4w32a	1%	70.94	91.22
+RES+CLC	4w32a	1%	71.25	91.39

C. Ablation Studies

1) *Effect of Different Components*: Table III demonstrates the impact of different components (RES and CLC) on the performance of the quantized MobileNetV2 model on the CIFAR-100 dataset. It is evident from the table that using either RES or CLC alone can significantly improve the Top-1 and Top-5 accuracy of the model. However, the most substantial performance gains are achieved when both components are combined. Specifically, under the 2-bit weight quantization and 32-bit full-precision activation setting, using RES alone can increase the Top-1 accuracy from 46.84% to 48.77% and the Top-5 accuracy from 78.09% to 78.94%. Using CLC alone can boost the Top-1 accuracy to 55.25% and the Top-5 accuracy to 84.03%. When both RES and CLC are used together, the Top-1 accuracy further increases to 56.36% and the Top-5 accuracy to 85.08%. This indicates that RES and CLC are complementary in reducing quantization errors, and their combined use can more effectively enhance the performance of quantized models.

TABLE IV: Coreset selection metric analysis. We report the Top-1 and Top-5 accuracy of quantized MobileNetV2 on CIFAR-100.

Model	d_{EVS}	d_{DS}	d_{RES}	Top-1	Top-5
MobileNetV2	✓			53.87	82.44
		✓		54.05	82.79
			✓	55.41	83.23
	✓	✓		55.25	84.03
	✓		✓	56.18	84.25
	✓	✓	✓	55.33	83.71
				56.36	85.08

The same trend persists under higher bitwidth quantization settings. For instance, under the 3-bit weight quantization and 32-bit full-precision activation setting, using RES alone can increase the Top-1 accuracy from 64.98% to 65.90% and the Top-5 accuracy from 88.64% to 89.29%. Using CLC alone can boost the Top-1 accuracy to 68.32% and the Top-5 accuracy to 90.53%. When both RES and CLC are combined, the Top-1 accuracy further increases to 68.69% and the Top-5 accuracy to 90.89%. This further proves the effectiveness of RES and CLC across different quantization bitwidths.

2) *Effect of Coreset Selection Metric*: Table IV provides a detailed analysis of the impact of different coreset selection metrics on the performance of the quantized MobileNetV2 model on the CIFAR-100 dataset. The results demonstrate that the choice of selection metric plays a crucial role in determining the effectiveness of the coreset in capturing the essential features of the dataset and, consequently, the performance of the quantized model. Specifically, the table shows the performance of the model when using individual metrics (d_{EVS} , d_{DS} , and d_{RES}) as well as their combinations.

When using a single metric for coreset selection, d_{RES} (Relative Entropy Score) achieves the highest Top-1 accuracy of 55.42%, outperforming the other individual metrics. This indicates that d_{RES} is particularly effective in capturing the

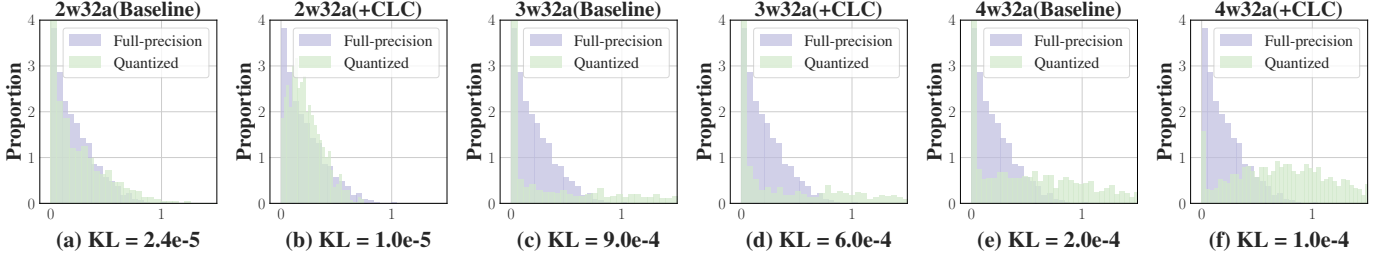


Fig. 3: Comparison of the selected inter-layer output distributions between the full-precision MobileNetV2 model and the quantized model with different quantization settings on CIFAR-100.

quantization errors, which is a critical factor for improving the performance of the quantized model. The metric d_{RES} directly measures the difference between the output distributions of the quantized and full-precision models, making it a strong indicator of how well the coreset can represent the quantization errors. In contrast, d_{EVS} and d_{DS} focus on gradient-based selection, which is also important but less effective on its own in capturing the quantization errors. For example, using d_{EVS} alone results in a Top-1 accuracy of 53.87%, while d_{DS} alone achieves 54.05%. Although these metrics are useful for identifying samples that contribute significantly to the gradient updates, they do not directly address the quantization errors, which are the primary source of performance degradation in quantized models. The most significant performance improvement is observed when all three metrics (d_{EVS} , d_{DS} , and d_{RES}) are combined. The combined metric achieves a Top-1 accuracy of 56.36%, which is higher than any individual metric. This suggests that a comprehensive coreset selection strategy that considers both gradient information and quantization errors is more effective in improving the performance of the quantized model. The combined metric leverages the strengths of each individual metric: d_{EVS} and d_{DS} provide information about the gradient updates, while d_{RES} ensures that the coreset captures the quantization errors effectively. By integrating these aspects, the coreset becomes more representative of the full dataset, leading to better training efficiency and higher accuracy of the quantized model.

3) *Visualization of Inter-layer Output*: Fig. 3 illustrates the distribution of intermediate layer outputs for the quantized and full-precision models, highlighting the effectiveness of the proposed Cascaded Layer Correction (CLC) strategy in reducing quantization errors across different quantization bitwidth settings. The figure compares the output distributions of the selected intermediate layer (the second-to-last layer) of MobileNetV2 on the CIFAR-100 dataset, with weights quantized to 2/3/4-bit precision, while activations remain in full precision. The KL divergence values shown in each subplot indicate the difference between the output distributions of the quantized and full-precision models.

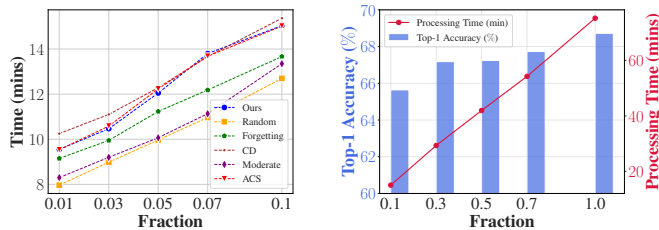
In the case of 2-bit weight quantization, the baseline quantized model exhibits a KL divergence of $2.4\text{e-}5$ compared to the full-precision model. After applying the CLC strategy, the KL divergence is reduced to $1.0\text{e-}5$, indicating significant alignment of the output distributions. This demonstrates that the CLC strategy effectively mitigates the quantization errors

TABLE V: The results of combining CLC with different coreset selection methods. we report the Top-1 and Top-5 accuracy of quantized MobileNetV2 on CIFAR-100.

Method	Bit width	Fraction	Top-1	Top-5
Random	2w32a	1%	40.57	71.74
Random+CLC	2w32a	1%	49.32	79.01
Forgetting	2w32a	1%	40.73	70.69
Forgetting+CLC	2w32a	1%	47.29	77.96
CD	2w32a	1%	38.61	68.30
CD+CLC	2w32a	1%	48.53	78.59
Moderate	2w32a	1%	35.14	65.47
Moderate+CLC	2w32a	1%	46.40	78.21
ACS	2w32a	1%	46.84	78.09
ACS+CLC	2w32a	1%	55.25	84.03

introduced by low-bit weight precision. For 3-bit weight quantization, the baseline KL divergence is $9.0\text{e-}4$. However, the CLC strategy reduces this divergence to $6.0\text{e-}4$. Similarly, for 4-bit weight quantization, the baseline KL divergence is $2.0\text{e-}4$, and the CLC strategy further reduces it to $1.0\text{e-}4$. The consistent reduction in KL divergence across different quantization bitwidths confirms the effectiveness of the CLC strategy in aligning intermediate layer outputs, thereby improving the overall accuracy and performance of the quantized model.

4) *CLC with Different Coreset Selection Methods*: Table V provides a comprehensive evaluation of the CLC strategy when integrated with various coreset selection methods. The results highlight the versatility and effectiveness of the CLC approach in enhancing the performance of quantized models across different coreset selection techniques. Specifically, the combination of CLC with the Random achieves an 8.75% improvement in performance. This significant enhancement demonstrates that even a simple random selection of coreset can benefit substantially from the CLC strategy, which effectively mitigates the quantization errors in intermediate layers. Similarly, when CLC is combined with Forgetting, the performance improves by 6.56%. The effectiveness of CLC is further underscored by its combination with other coreset selection methods. For instance, integrating CLC with CD results in a 9.92% performance improvement, while combining it with Moderate method yields an 11.26% enhancement. These results suggest that CLC can significantly boost the performance of quantized models regardless of the coreset selection method used. When CLC is combined with ACS,



(a) Comparison of Efficiency. (b) Time-Accuracy Analysis.

Fig. 4: (a) The efficiency of different methods. (b) Balance between efficiency and accuracy of our method. The experimental setup is 2-bit quantized MobileNetV2 on CIFAR-100.

the performance improvement reaches 8.41%. This highlights the robustness of CLC in enhancing model performance, as ACS is already an advanced method that selects samples based on their impact on gradients. Overall, the CLC strategy is highly adaptable and can effectively improve the performance of quantized models when combined with various coreset selection methods.

5) *Efficiency Analysis*: We compare the efficiency of different methods, as shown in Fig. 4(a). Random demonstrates the highest efficiency, taking only 7.97 minutes to train on 1% of the data. However, despite its significant time-saving advantage, Random suffers from severe performance degradation due to the randomness in selecting the coreset. Specifically, Forgetting takes 9.15 minutes, Moderate takes 8.30 minutes, ACS takes 9.53 minutes, and our method takes 9.55 minutes. Although our method is slightly slower than ACS, it is faster than CD (10.25 minutes). More importantly, our method can significantly improve model performance while maintaining high efficiency. This indicates that our method achieves a good balance between efficiency and performance, avoiding the significant performance drop caused by the Random and Moderate methods' overemphasis on efficiency and overcoming the low efficiency of CD method. Our method provides an effective solution for efficient and high-performance model training on small-scale coresets.

We further analyze the balance between efficiency and accuracy for our method. As shown in Fig. 4(b), when training with 20% of the data, our method takes 29.32 minutes and achieves a Top-1 accuracy of 67.18%. In contrast, training with the full dataset (100%) takes 75.22 minutes, resulting in a Top-1 accuracy of 68.72%. The time cost increases by 157%, but the accuracy only improves by 1.54%. This indicates that using a small fraction of the data (e.g., 20%) with our method can achieve a significant reduction in training time while maintaining a high level of accuracy. The marginal gain in accuracy from increasing the data fraction beyond 20% is relatively small compared to the substantial increase in training time. Therefore, our method provides an effective trade-off between efficiency and accuracy, especially when computational resources are limited or when faster training is desired without significant loss in model performance.

6) *Effect of Larger Fractions*: To provide a more comprehensive validation of our method, we present results with

TABLE VI: Results with larger fractions. we report the Top-1 and Top-5 accuracy of quantized MobileNetV2 on CIFAR-100. The full-precision MobileNetV2 achieves a Top-1 accuracy of 72.56% and a Top-5 accuracy of 91.93% on CIFAR-100.

Method	Bit width	Fraction	Top-1	Top-5
ACS	2w32a	20%	65.03	89.14
Ours	2w32a	20%	65.86	89.70
ACS	2w32a	30%	66.32	89.19
Ours	2w32a	30%	67.18	90.53
ACS	2w32a	50%	67.13	90.28
Ours	2w32a	50%	67.24	90.50
ACS	2w32a	70%	67.51	90.06
Ours	2w32a	70%	67.73	91.01
ACS	2w32a	100%	67.67	90.31
Ours	2w32a	100%	68.72	91.21

TABLE VII: Results with different teacher models. The student model is the quantized ResNet-18 with both weights and activations quantized to 2-bit. We report the Top-1 accuracy.

Teacher	ResNet-18	ResNet-34	ResNet-101
Top-1(%)	46.24	46.27	46.34

larger fractions. As shown in Table VI, our approach continues to demonstrate superior performance compared to the current state-of-the-art method, ACS, even at larger fractions. At smaller data fractions (such as 20% and 30%), our method outperforms ACS in terms of both Top-1 and Top-5 accuracy, achieving improvements of 0.83% and 0.86% in Top-1 accuracy, and 0.56% and 1.34% in Top-5 accuracy, respectively. This demonstrates that our method can more effectively utilize limited samples for training when data is restricted, thereby enhancing model performance. However, as the data fraction increases, the magnitude of performance improvement gradually diminishes. At a 50% data fraction, the Top-1 accuracy is improved by only 0.11%, and the Top-5 accuracy by 0.22%; while at a 100% data fraction, the Top-1 accuracy is enhanced by 1.05%, and the Top-5 accuracy by 0.90%. This phenomenon indicates that when the data volume approaches full-data training, the room for model performance improvement is relatively limited. Nevertheless, our method still manages to deliver certain performance gains, which further proves its effectiveness across different data scales.

7) *Effect of Different Teacher Models*: For the ResNet-18 model on ImageNet-1K, we demonstrate the impact of different teacher models on the results. As shown in Table VII, more complex teacher models can guide the student model to achieve better performance. Specifically, when using ResNet-101 as the teacher model, the Top-1 accuracy of the quantized ResNet-18 with both weights and activations quantized to 2-bit reaches 46.34%, which is slightly higher than that achieved with ResNet-34 as the teacher model at 46.27% and ResNet-18 as the teacher model at 46.24%. This indicates that during the knowledge distillation process, more complex teacher models can provide more informative guidance for the student model, thereby enhancing the performance of the quantized model.



Fig. 5: UAV prototype.

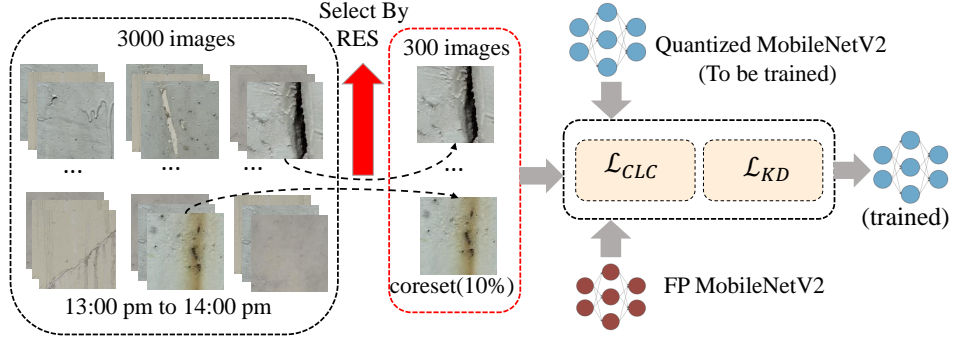


Fig. 6: The process of coreset selection and quantized model training.

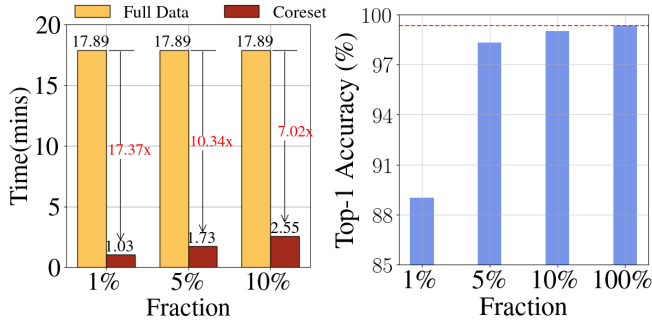


Fig. 7: Analysis of Top-1 Accuracy and Training Time.

VI. A CASE STUDY

We evaluate QuaRC on a UAV-based crack-detection task for infrastructure inspection. In this setting, UAVs equipped with onboard vision systems must run lightweight quantized models under tight compute and energy budgets. To accommodate bridge- and building-specific variations in crack morphology and lighting—and to avoid transmitting sensitive inspection images to the cloud—quantized models must be retrained locally using newly captured data. However, full-dataset QAT onboard is infeasible on resource-constrained hardware. By selecting a small, representative subset (1–10% of data), QuaRC enables rapid on-device retraining of quantized models without degrading detection accuracy.

Figure 5 shows our UAV platform, which integrates an NVIDIA Jetson Orin NX 16 GB edge module and a Homer digital link (1.5 km range). We begin by uploading full-precision MobileNetV2 weights (pretrained on ImageNet-1K) to the UAV. The UAV then acquires 3,300 concrete-surface images (3,000 for training, 300 for testing) over a one-hour flight and annotates cracks offline. As depicted in Figure 6, we first fine-tune the full-precision model for 20 epochs on all 3,000 images, achieving 99.33% Top-1 accuracy. Next, we run the RES algorithm to select the 300 most informative images (10%), then retrain the 2-bit quantized MobileNetV2 with our Cascaded Layer Correction strategy. As shown in Figure 7, this coreset QAT completes in 2.55 minutes—7.02× faster than full-dataset QAT—while delivering 99.00% Top-1 accuracy (vs. 99.33% on the full dataset). These results

confirm that QuaRC substantially accelerates on-device QAT while preserving model performance.

VII. RELATED WORK AND DISCUSSION

In this section, we first introduce the relevant studies on integrating coreset selection methods with QAT from the aspects of *model quantization* and *coreset selection*. Subsequently, we discuss the limitations and potential extensions of QuaRC.

A. Related Work

Model quantization: As one of the key technologies for deep learning model compression, model quantization [7], [35], [36] aims to reduce computational costs and memory usage by converting full-precision floating-point numbers into low-bit integers, thereby enabling models to be deployed on resource-constrained hardware. Quantization methods are categorized into Post-Training Quantization (PTQ) [8], [9] and Quantization-Aware Training (QAT) [10], [11], with QAT showing better performance for extremely low bitwidths (4 bits or fewer). Techniques like Dorefa-net [10] focus on accelerating training and inference with low bitwidth parameters, while LSQ [11] and LSQ+ [34] use learnable quantization parameters to achieve better accuracy. Although QAT provides superior performance, it requires retraining on the entire dataset, increasing computational costs. Our work focuses on reducing the computational overhead of QAT so that it can be applied to resource-constrained edge devices.

Coreset selection: By selecting a subset that can represent the key features of the entire dataset, coreset selection techniques can improve training efficiency, reduce the demand for computational resources, and maintain model performance. Common methods for evaluating sample importance in coreset selection include geometry-based [25], [26], decision boundary-based [37], [38], and gradient-based [13], [39] approaches. These coreset selection methods are designed for full-precision models and do not consider the characteristics of quantized models. Fortunately, ACS [16] considers the impact of samples on the quantized model from the perspective of gradients, and for the first time, applies coreset selection to QAT. Due to the consideration of quantization characteristics, the performance of ACS is significantly better than traditional methods. Unlike ACS, we approach from the perspective of quantization errors,

selecting the samples that best reflect the model’s quantization errors as the coreset.

Applying coreset selection to QAT can enhance its training efficiency. However, when using a small-scale coreset for QAT, there can be a notable decline in the performance of the quantized model. Our work aims to **mitigate this performance degradation of the quantized model when employing a small-scale coreset for QAT.**

B. Discussion

Limitations: Despite the significant improvements achieved by QuaRC in QAT on small-scale coresets, there are still some limitations. First, the calculation of the RES requires both the full-precision model and the quantized model to perform inference on all samples simultaneously, which introduces additional computational overhead during the coreset selection phase. Although the overhead is significantly reduced compared to the backpropagation process, it can still be a bottleneck for edge devices with extremely limited resources. Second, the CLC strategy demands that the full-precision correction model be strictly aligned in structure with the quantized model. If the teacher model and the correction model are not consistent, the training cost will increase. Experiments have shown that although using a deeper teacher model can slightly improve accuracy, the optimal solution for on-device training is to set the teacher model and the correction model as the same model, thereby achieving the best balance between accuracy and efficiency.

Potential Extensions: While our current work focuses on enhancing quantization-aware training for image classification models, the principles underlying QuaRC—quantization error-aware coreset selection and intermediate layer correction—exhibit promising potential for broader applications. RES selects the coreset by capturing quantization errors, and its nature is task-agnostic, allowing it to be easily adapted to other visual tasks such as object detection [40], [41] and semantic segmentation [42], [43]. CLC mitigates error accumulation by aligning intermediate features layer-by-layer and is equally applicable to the quantization training of hierarchical network architectures, such as those based on the Transformer framework [44], [45]. However, the current limitations in computational power and memory on edge devices still pose significant challenges for local training of object detection models and large models based on the Transformer architecture. Nevertheless, with the continuous advancement of edge computing hardware, the computational bottlenecks on edge devices are expected to be gradually overcome. Against this backdrop, our future work will focus on the aforementioned directions, aiming to facilitate the implementation of efficient quantization-aware training techniques on edge devices.

VIII. CONCLUSION

This paper proposes an innovative solution, QuaRC, to address the core challenge of Quantization-Aware Training (QAT) on edge devices: the accumulation of quantization errors when using small-scale coresets. In our research, we delve into two major challenges encountered when applying

coreset selection to QAT: 1) the failure to consider quantization errors during coreset selection, and 2) the difficulty in eliminating intermediate layer errors in the quantized model during the training phase. To tackle these challenges, we introduce the Relative Entropy Score as the selection metric in the coreset selection stage and employ the Cascaded Layer Correction strategy during the training phase of the quantized model to eliminate errors in the intermediate layers. Extensive experiments demonstrate the significant advantages of our proposed method over existing approaches. Our work effectively mitigates the performance degradation of quantized models when using small-scale coresets, thereby making it possible to perform QAT directly on edge devices.

REFERENCES

- [1] G. Cheng, J. Han, and X. Lu, “Remote sensing image scene classification: Benchmark and state of the art,” *Proceedings of the IEEE*, vol. 105, no. 10, pp. 1865–1883, 2017.
- [2] H. Zakeri, F. M. Nejad, and A. Fahimifar, “Image based techniques for crack detection, classification and quantification in asphalt pavement: a review,” *Archives of Computational Methods in Engineering*, vol. 24, pp. 935–977, 2017.
- [3] M. M. H. Shuvo, S. K. Islam, J. Cheng, and B. I. Morshed, “Efficient acceleration of deep learning inference on resource-constrained edge devices: A review,” *Proceedings of the IEEE*, vol. 111, no. 1, pp. 42–91, 2022.
- [4] T. Zhao, Y. Xie, Y. Wang, J. Cheng, X. Guo, B. Hu, and Y. Chen, “A survey of deep learning on mobile devices: Applications, optimizations, challenges, and research opportunities,” *Proceedings of the IEEE*, vol. 110, no. 3, pp. 334–354, 2022.
- [5] A. G. Howard, M. Zhu, B. Chen, D. Kalenichenko, W. Wang, T. Weyand, M. Andreetto, and H. Adam, “Mobilenets: Efficient convolutional neural networks for mobile vision applications,” *arXiv preprint arXiv:1704.04861*, 2017.
- [6] R. Chen, L. Li, K. Xue, C. Zhang, M. Pan, and Y. Fang, “Energy efficient federated learning over heterogeneous mobile devices via joint design of weight quantization and wireless transmission,” *IEEE Transactions on Mobile Computing (TMC)*, vol. 22, no. 12, pp. 7451–7465, 2022.
- [7] F. Luo, A. Li, S. Khan, K. Wu, and L. Wang, “Bi-deepvit: Binarized transformer for efficient sensor-based human activity recognition,” *IEEE Transactions on Mobile Computing (TMC)*, 2025.
- [8] J. Fang, A. Shafiee, H. Abdel-Aziz, D. Thorsley, G. Georgiadis, and J. H. Hassoun, “Post-training piecewise linear quantization for deep neural networks,” in *Computer Vision—ECCV 2020: 16th European Conference, Glasgow, UK, August 23–28, 2020, Proceedings, Part II 16*. Springer, 2020, pp. 69–86.
- [9] P. Wang, Q. Chen, X. He, and J. Cheng, “Towards accurate post-training network quantization via bit-split and stitching,” in *International Conference on Machine Learning*. PMLR, 2020, pp. 9847–9856.
- [10] S. Zhou, Y. Wu, Z. Ni, X. Zhou, H. Wen, and Y. Zou, “Dorefa-net: Training low bitwidth convolutional neural networks with low bitwidth gradients,” *arXiv preprint arXiv:1606.06160*, 2016.
- [11] S. K. Esser, J. L. McKinstry, D. Bablani, R. Appuswamy, and D. S. Modha, “Learned step size quantization,” in *International Conference on Learning Representations*, 2020.
- [12] M. Welling, “Herding dynamical weights to learn,” in *Proceedings of the 26th annual international conference on machine learning*, 2009, pp. 1121–1128.
- [13] M. Paul, S. Ganguli, and G. K. Dziugaite, “Deep learning on a data diet: Finding important examples early in training,” *Advances in neural information processing systems*, vol. 34, pp. 20 596–20 607, 2021.
- [14] K. Killamsetty, S. Durga, G. Ramakrishnan, A. De, and R. Iyer, “Grad-match: Gradient matching based data subset selection for efficient deep model training,” in *International Conference on Machine Learning*. PMLR, 2021, pp. 5464–5474.
- [15] B. Sorscher, R. Geirhos, S. Shekhar, S. Ganguli, and A. Morcos, “Beyond neural scaling laws: beating power law scaling via data pruning,” *Advances in Neural Information Processing Systems*, vol. 35, pp. 19 523–19 536, 2022.
- [16] X. Huang, Z. Liu, S.-Y. Liu, and K.-T. Cheng, “Robust and efficient quantization-aware training via coreset selection,” *Transactions on Machine Learning Research*, 2024.

- [17] Y. Li, S. Xu, B. Zhang, X. Cao, P. Gao, and G. Guo, "Q-vit: Accurate and fully quantized low-bit vision transformer," *Advances in neural information processing systems*, vol. 35, pp. 34451–34463, 2022.
- [18] M. Nagel, M. Fournarakis, Y. Bondarenko, and T. Blankevoort, "Overcoming oscillations in quantization-aware training," in *International Conference on Machine Learning*. PMLR, 2022, pp. 16318–16330.
- [19] Y. Bengio, N. Léonard, and A. Courville, "Estimating or propagating gradients through stochastic neurons for conditional computation," *arXiv preprint arXiv:1308.3432*, 2013.
- [20] C.-F. R. Chen, Q. Fan, and R. Panda, "Crossvit: Cross-attention multi-scale vision transformer for image classification," in *Proceedings of the IEEE/CVF international conference on computer vision*, 2021, pp. 357–366.
- [21] A. Mishra and D. Marr, "Apprentice: Using knowledge distillation techniques to improve low-precision network accuracy," in *International Conference on Learning Representations*, 2018. [Online]. Available: <https://openreview.net/forum?id=B1ae1IZRb>
- [22] X. Huang, Z. Shen, S. Li, Z. Liu, H. Xianghong, J. Wicaksana, E. Xing, and K.-T. Cheng, "Sdq: Stochastic differentiable quantization with mixed precision," in *International Conference on Machine Learning*. PMLR, 2022, pp. 9295–9309.
- [23] A. Mishra and D. Marr, "Apprentice: Using knowledge distillation techniques to improve low-precision network accuracy," *arXiv preprint arXiv:1711.05852*, 2017.
- [24] S.-Y. Liu, Z. Liu, and K.-T. Cheng, "Oscillation-free quantization for low-bit vision transformers," in *International Conference on Machine Learning*. PMLR, 2023, pp. 21813–21824.
- [25] X. Xia, J. Liu, J. Yu, X. Shen, B. Han, and T. Liu, "Moderate coreset: A universal method of data selection for real-world data-efficient deep learning," in *The Eleventh International Conference on Learning Representations*, 2023. [Online]. Available: <https://openreview.net/forum?id=7D5EECbOaf9>
- [26] S. Agarwal, H. Arora, S. Anand, and C. Arora, "Contextual diversity for active learning," in *Computer Vision—ECCV 2020: 16th European Conference, Glasgow, UK, August 23–28, 2020, Proceedings, Part XVI 16*. Springer, 2020, pp. 137–153.
- [27] M. Toneva, A. Sordoni, R. T. des Combes, A. Trischler, Y. Bengio, and G. J. Gordon, "An empirical study of example forgetting during deep neural network learning," in *International Conference on Learning Representations*, 2019. [Online]. Available: <https://openreview.net/forum?id=BJlXm30cKm>
- [28] H. Li, X. Wu, F. Lv, D. Liao, T. H. Li, Y. Zhang, B. Han, and M. Tan, "Hard sample matters a lot in zero-shot quantization," in *Proceedings of the IEEE/CVF conference on Computer Vision and Pattern Recognition*, 2023, pp. 24417–24426.
- [29] S. Li, Y. Zhao, R. Varma, O. Salpekar, P. Noordhuis, T. Li, A. Paszke, J. Smith, B. Vaughan, P. Damania, and S. Chintala, "Pytorch distributed: Experiences on accelerating data parallel training," *CoRR*, vol. abs/2006.15704, 2020.
- [30] A. Krizhevsky, G. Hinton *et al.*, "Learning multiple layers of features from tiny images," 2009.
- [31] J. Deng, W. Dong, R. Socher, L.-J. Li, K. Li, and L. Fei-Fei, "Imagenet: A large-scale hierarchical image database," in *2009 IEEE conference on computer vision and pattern recognition*. Ieee, 2009, pp. 248–255.
- [32] A. Paszke, S. Gross, F. Massa, A. Lerer, J. Bradbury, G. Chanan, T. Killeen, Z. Lin, N. Gimesheine, L. Antiga *et al.*, "Pytorch: An imperative style, high-performance deep learning library," *Advances in neural information processing systems*, vol. 32, 2019.
- [33] K. He, X. Zhang, S. Ren, and J. Sun, "Deep residual learning for image recognition," in *Proceedings of the IEEE conference on computer vision and pattern recognition*, 2016, pp. 770–778.
- [34] Y. Bhalgat, J. Lee, M. Nagel, T. Blankevoort, and N. Kwak, "Lsq+: Improving low-bit quantization through learnable offsets and better initialization," in *Proceedings of the IEEE/CVF conference on computer vision and pattern recognition workshops*, 2020, pp. 696–697.
- [35] C. Yang, J. Yuan, Y. Wu, Q. Sun, A. Zhou, S. Wang, and M. Xu, "Communication-efficient satellite-ground federated learning through progressive weight quantization," *IEEE Transactions on Mobile Computing (TMC)*, vol. 23, no. 9, pp. 8999–9011, 2024.
- [36] F. Luo, S. Khan, Y. Huang, and K. Wu, "Binarized neural network for edge intelligence of sensor-based human activity recognition," *IEEE transactions on mobile computing (TMC)*, vol. 22, no. 3, pp. 1356–1368, 2021.
- [37] M. Ducoffe and F. Precioso, "Adversarial active learning for deep networks: a margin based approach," *arXiv preprint arXiv:1802.09841*, 2018.
- [38] K. Margatina, G. Vernikos, L. Barrault, and N. Aletras, "Active learning by acquiring contrastive examples," in *Proceedings of the 2021 Conference on Empirical Methods in Natural Language Processing*, 2021, pp. 650–663.
- [39] B. Mirzasoleiman, J. Bilmes, and J. Leskovec, "Coresets for data-efficient training of machine learning models," in *International Conference on Machine Learning*. PMLR, 2020, pp. 6950–6960.
- [40] Z.-Q. Zhao, P. Zheng, S.-t. Xu, and X. Wu, "Object detection with deep learning: A review," *IEEE transactions on neural networks and learning systems*, vol. 30, no. 11, pp. 3212–3232, 2019.
- [41] Z. Zou, K. Chen, Z. Shi, Y. Guo, and J. Ye, "Object detection in 20 years: A survey," *Proceedings of the IEEE*, vol. 111, no. 3, pp. 257–276, 2023.
- [42] Y. Mo, Y. Wu, X. Yang, F. Liu, and Y. Liao, "Review the state-of-the-art technologies of semantic segmentation based on deep learning," *Neurocomputing*, vol. 493, pp. 626–646, 2022.
- [43] H. Thisanake, C. Deshan, K. Chamith, S. Seneviratne, R. Vidanaarachchi, and D. Herath, "Semantic segmentation using vision transformers: A survey," *Engineering Applications of Artificial Intelligence*, vol. 126, p. 106669, 2023.
- [44] J. Devlin, M.-W. Chang, K. Lee, and K. Toutanova, "Bert: Pre-training of deep bidirectional transformers for language understanding," in *Proceedings of the 2019 conference of the North American chapter of the association for computational linguistics: human language technologies, volume 1 (long and short papers)*, 2019, pp. 4171–4186.
- [45] T. Brown, B. Mann, N. Ryder, M. Subbiah, J. D. Kaplan, P. Dhariwal, A. Neelakantan, P. Shyam, G. Sastry, A. Askell *et al.*, "Language models are few-shot learners," *Advances in neural information processing systems*, vol. 33, pp. 1877–1901, 2020.